Structural organization of phosphorus titanate oxides prepared by the alkoxo method and their catalytic activity in ethylene glycol oxyethylation

R. A. Kozlovskii,[a] V. V. Yushchenko,[b] L. E. Kitaev,[b] O. V. Bukhtenko,[c] A. M. Voloshchuk,[d] L. N. Vasil´eva,[e] and M. V. Tsodikov[c]★

[a]*D. I. Mendeleev Russian Chemico-Technological University , 9 Miusskaya pl., 125047 Moscow, Russian Federation. Fax: +7 (095) 978 9554*

[b]*Department of Chemistry, M. V. Lomonosov Moscow State University, Leninskie Gory, 119899 Moscow, Russian Federation. Fax: +7 (095) 932 8846*

[c]*A. V. Topchiev Institute of Petrochemical Synthesis, Russian Academy of Sciences, 29 Leninsky prosp., 119991 Moscow, Russian Federation. Fax +7 (095) 234 3232. E-mail: tsodikov@ips.ac.ru*

[d]*Institute of Physical Chemistry, Russian Academy of Sciences, 31 Leninsky prosp., 119991 Moscow, Russian Federation. Fax: +7 (095) 952 5308*

[e]*Department of Chemistry, Moscow State Pedagogical University, 1 ul. M. Pirogovskaya, 117915 Moscow, Russian Federation. Fax: +7 (095) 246 7766*

The relationship of the structural organization and acid-base properties of the surface of phosphorus titanate oxides prepared from tetra-*n*-butoxytitanium and phosphorous esters with the catalytic activity and selectivity of these materials in ethylene glycol oxyethylation was studied. Single-phase phosphorus-containing oxides synthesized from 2-diethylamido-4-methyl-1,3,2-dioxophosphorinane and diphenyl(methano)phosphocane have strong surface aprotic acid sites and exhibit high catalytic activity with respect to oxyethylation and a record-breaking selectivity in the formation of the lower homolog, diethylene glycol. The last-mentioned fact is a consequence of the sieve effect exerted by the homogeneous porous structure of supermicropores (8—10 Å) of the oxides. An increase in the concentration of the strong acid sites (≥130 kJ mol^{-1}) on the oxide surface enhances the catalytic activity. On the basis of the temperature programmed desorption of ammonia and CO_2 and kinetic measurements, a concerted acid-base mechanism was proposed for the catalytic addition of ethylene oxide to ethylene glycol on the phosphorus-titanate surface.

Key words: alkoxo method, tetra-*n*-butoxytitanium, phosphorous esters, structure, porosity, X-ray diffraction, temperature programmed desorption, ammonia, carbon dioxide, regional rate method, catalysis, oxyethylation of ethylene glycol, catalytic activity, selectivity.

The reactions of ethylene oxide (EO) with alcohols and glycols underlie industrial processes for the production of valuable products, *viz.*, cellosolves, carbitols, nonionic surfactants, and polyethers. Most often, these processes occur in the presence of homogeneous alkaline catalysts.[1—3] In some cases, homogeneous Lewis acids are employed.[1—3] The main drawback of the acid catalysts is the formation of a by-product (dioxane).[1,4] A common disadvantage of homogeneous catalysts is the difficulty of separating them from the reaction products. Therefore, the search for active and selective heterogeneous catalysts is in progress.

The addition of ethylene oxide to alcohols (oxyethylation) is a consecutive-parallel reaction

$$ROH \xrightarrow[k_0]{C_2H_4O} ROCH_2CH_2OH \xrightarrow[k_1]{C_2H_4O} RO(H_2CH_2O)_2 \xrightarrow[k_2]{C_2H_4O} \ldots$$

The composition of the reaction products depends on the ratio of the rate constants for the subsequent steps to the rate constant for the first oxyethylation step, which is called the distribution coefficient[5] $C_i = k_i/k_0$.

Published in Russian in *Izvestiya Akademii Nauk. Seriya Khimicheskaya,* No. 6, pp. 887—893, June, 2002.

1066-5285/02/5106-967 $27.00

The distribution coefficients are usually $C_1 \approx 2$; $C_2 \approx 3$ for base catalysts[5,6] and $C_1 \approx C_2 \approx \ldots C_i \approx 1$ for acid catalysts.[4] From the practical standpoint, the catalysts that ensure low distribution coefficients and provide higher yields of individual glycol ethers are the most efficient.

Previously,[7,8] we showed that phosphorus titanate oxides prepared by the alkoxo method using etriol phosphite and tetra-*n*-butoxytitanium as precursors possess a highly organized structure and that variation of the synthesis conditions allows one to change their acid-base properties.

In this work, we studied the influence of the nature of phosphorous esters used as the precursors, together with tetra-*n*-butoxytitanium, on the structural organization of the oxides, the acid-base properties of their surface, and the catalytic activity in oxyethylation of ethylene glycol.

Experimental

Phosphorus titanate oxides **1—10** were prepared by the alkoxo method according to a known procedure.[7] An equimolar amount of acetylacetone was added to a 1.5 *M* solution of tetra-*n*-butoxytitanium in anhydrous benzene. After stirring for 30 min, a specified amount (2% based on the oxide) of a phosphite was added under Ar to the resulting solution of titanium alkoxide. The phosphites included 2-diethylamido-4-methyl-1,3,2-dioxaphosphorinane ($C_4H_{18}O_2PN$) (**1a**), diethylamido(2,2′-dioxa-5,5′-dimethyl-1,1′-diphenylmethano)phosphocane (**2a**) and 1 : 1 complexes of CuBr with them (**3a** and **4a**, respectively), described previously.[9,10] The resulting sol was stirred for 30 min and then diluted with aqueous alcohol containing water in a stoichiometric amount with respect to the alkoxide complex. The gel was isolated by evaporating the solvents on a rotary evaporator, dried in air and *in vacuo*, and subjected to a stepwise heat treatment for 2 h at 200, 2 h at 300 °C, and 6 h at 500 °C. This gave specimens **1—4**. For comparison, nonmodified TiO_2 oxides with the anatase (**5**) and rutile (**6**) structures were synthesized by the alkoxo method. Oxides containing 2% Al and Cu ions (specimens **7** and **8**) were prepared from inorganic precursors, CuBr and $Al_2(SO_4)_3 \cdot 18H_2O$. Titanium oxide (rutile) was synthesized by hydrolysis of tetra-*n*-butoxytitanium without the addition of acetylacetone followed by heat treatment of the gel at 550 °C. In the syntheses of specimens **7** and **8**, the inorganic precursors as solutions in aqueous alcohol were added to a benzene solution of alkoxide preliminarily chelated by acetylacetone. Upon the addition of aluminum sulfate (sample **8**), the initial solution grew turbid due to the formation of a highly dispersed gel; the solution was refluxed for 2 h and then, as in the syntheses of samples **1—7**, the gel was isolated by evaporating the solvent, dried, and annealed.

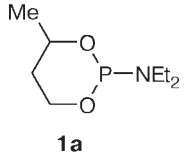

1a

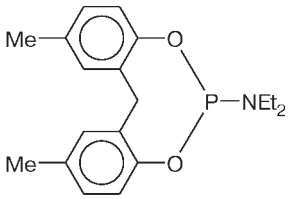

2a

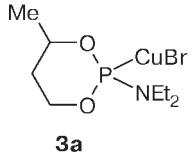

3a

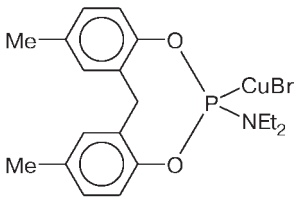

4a

The catalytic activity of titanate oxides in the oxyethylation of ethylene glycol (EG) was studied using a pressure-gauge setup;[11] the reaction rate was monitored by a decrease in the ethylene oxide vapor pressure. The large molar excess of the alcohol ensured pseudo-first-order reaction conditions: $r = k_{app}p_{EO}$, where p_{EO} is the partial pressure of EO. The experimental rate constant was found as the slope ratio of the straight line plotted in the $\ln(p_{EO})$—time coordinates. Since a noncatalytic reaction takes place in the reaction mixture in parallel to the catalyzed reaction, then, with the assumption of the first order with respect to the catalyst

$$r = (k_{noncat} + k_{cat}^{*}[\text{Cat.}])p_{EO}, \qquad (1)$$

the catalytic rate constant (k_{cat}) was found from the relation

$$k_{cat} = (k_{app} - k_{noncat})/[\text{Cat.}],$$

where k_{noncat} is the rate constant for the noncatalytic reaction; [Cat.] is the catalyst concentration. The composition of the reaction products was studied by GLC on a Khrom-5 instrument (flame ionization detector, a 1 m×4 mm glass packed column, 15% FFAP on Inerton AW HMDC, nitrogen as the carrier gas). The temperature of the column thermostat was programmed from 120 to 230 °C at a rate of 25 K min^{-1}.

The distribution coefficients (*C*) were determined by solving a Weibull—Nycander set of equations[12] used to describe the product composition in the case where $k_0 \neq k_1 = k_2 = \ldots$:

$$[HOCH_2CH_2O(CH_2CH_2O)_nH] =$$
$$= -[HOCH_2CH_2OH]^C\left(\frac{C^{n-1}}{S[HOCH_2CH_2OH]_0^S}\sum_{i=0}^{n-1}\frac{1}{S^{n-1-i}}\frac{z^i}{i!}\right) +$$
$$+ \left(\frac{C^{n-1}}{S^n}\right)[HOCH_2CH_2OH],$$

where the molar concentrations are given in square brackets, $C = k_n/k_0$ is the distribution coefficient (the ratio of the rate constants for the subsequent steps to the rate constant for the first step), $S = C - 1$ for $C \neq 1$, $z = \ln[HOCH_2CH_2OH]_0/[HOCH_2CH_2OH]$.

The sum of squares of the differences between the calculated and experimental product compositions was minimized.

The selectivity of formation of the first product of EO addition, diethylene glycol (DEG) based on the initial EG was calculated by the equation

$$\Phi_{DEG}^{EG} = [DEG]/([EG]_0 - [EG]).$$

X-Ray diffraction analysis was carried out on a Dron-3M diffractometer using filtered Cu-Kα radiation. The phases were identified by comparison of the interplanar spacings and the relative intensities of Bragg reflections with the JCPDS-ICDD database (1987—1995). The crystal lattice parameters were calculated from the positions of lines characterizing the tetragonal orientation of the structure ([200] and [004]). The sample scan velocity was 0.5 deg min^{-1}. The fine structure, *viz.*, the size of microcrystallites (coherent scattering region) and structure microdistortions (ε), were determined from broadening of X-ray reflections.[13] To separate the dispersity and microdistortion effects, the calculations were carried out using two lines and preliminarily constructed nomographic charts, $m_1/\beta_1 = \Phi(\beta_2/\beta_1)$ and $n_2/\beta_2 = \Phi(\beta_2/\beta_1)$, where β_1 and β_2 are true physical broadenings of the lines with $d = 3.52$ and 1.89 Å, respectively, and m_1 and n_2 are the fractions of physical broadening caused by the block dispersity and microdistortions, respectively.

The parameters of the porous structure were found from the isotherms of nitrogen adsorption obtained at 77 K. Experimental adsorption isotherms were measured using an automated weighing setup (Netch, Germany) with a 1 μg sensitivity for a sample of up to 1 g at 77 K. The specific surface area was calculated by the BET method. The average pore size was determined with the assumption that the pores are slit-like. The homogeneity of the adsorption pores was assessed using a method[14] according to which an adsorption isotherm measured for a narrow-pore specimen is compared with an adsorption isotherm of a similar specimen characterized by wider pores. The theoretical adsorption isotherm in the a_{ads}—n coordinates, where a_{ads} is the adsorption pore volume and n is the number of adsorbed layers of sorbate molecules, was calculated by a semiempirical method in the whole range of relative pressures (p/p_s). The construction of the standard (reference) adsorption isotherm was based on the isotherm for the aluminum titanate oxide measured[7] for the monolayer range, while in the multilayer range, the isotherm was calculated by the BET method assuming the slit-like pores.[14]

In order to study the acid-base properties of the surface sites, temperature-programmed desorption of probe molecules, NH_3 and CO_2, was studied. The NH_3 and CO_2 temperature-programmed desorption (TPD) was carried out as follows. A sample (0.2 g) was annealed for 2 h at 550 °C in a dry air flow and for 1 h at the same temperature in a nitrogen flow, cooled, and purged with a nitrogen—ammonia mixture (1 : 1 v/v) for 0.5 h at ~20 °C or saturated with CO_2 for 0.5 h at ~20 °C. Then the loosely bound adsorbate was blown out for 1 h at 50 °C, the sample was cooled to ~20 °C, and the programmed heating at a rate of 8 K min^{-1} was carried out until the adsorbate was completely removed. The TPD data were processed by fitting the experimental and theoretical curves.[15] This made it possible to determine the total number of adsorption sites and the distribution function for these sites over the desorption activation energies (E_d) ranging from a minimum (E_{min}) to a maximum value (E_{max}) and to calculate the mean value ($\langle E \rangle$) over the whole desorption region, which characterizes the mean strength of the sites. The range of the desorption activation energies was split into equal sections (5 kJ mol^{-1} each), in which the sites were considered to be homogeneous, their strength being defined by the mean activation energy corresponding to the midpoint of the section.

Results and Discussion

X-Ray diffraction study of the modified titanate systems showed that the alkoxo synthesis yields single-phase oxides with an anatase structure. The titanium oxide prepared without the preliminary chelation step comprises the rutile (60%) and anatase (40%) modifications.

Table 1 presents the precursors and the structures of the phosphites used in the syntheses, the empirical formula of single-phase oxides determined from X-ray diffraction data and elemental composition, the rate constant for the catalytic reaction, and the distribution coefficient (C) characterizing the selectivity of titanate systems in the reaction. It can be seen that the nature of the precursors has a substantial effect on the catalytic activity of the oxides in ethylene glycol oxyethylation. Titanium oxide containing the rutile modification is inactive in oxyethylation. Titanium oxide with the anatase structure and the titanium—aluminum system (specimen **9**)

Table 1. Precursors, empirical formulas of oxides, and their catalytic properties in EG oxyethylation

Specimen	Precursor	Oxide formula	k_{cat} /L g^{-1} min^{-1}	C	Φ_{DEG}^{EG} *
1	**1a**	$P_{0.07}Ti_{0.91}O_{2-\delta}$	$1.28 \cdot 10^{-2}$	0.38	88.6
2	**2a**	$P_{0.07}Ti_{0.91}O_{2-\delta}$	$1.47 \cdot 10^{-2}$	0.51	85.5
3	**3a**	$Cu_{0.07}P_{0.07}Ti_{0.88}O_{2-\delta}$	$1.81 \cdot 10^{-3}$	0.52	85.5
4	**4a**	$Cu_{0.07}P_{0.07}Ti_{0.88}O_{2-\delta}$	$3.03 \cdot 10^{-3}$	0.37	88.9
5	TBT	TiO_2 (anatase)	$0.5 \cdot 10^{-5}$	0.9	78.6
6	TBT	TiO_2 (rutile+anatase)	—	—	
7	CuBr	$Cu_{0.04}Ti_{0.98}O_{2-\delta}$	$7.6 \cdot 10^{-4}$	—	
8	$Al_2(SO_4)_3 \cdot 18H_2O$	$Al_{0.09}Ti_{0.93}O_{2-\delta}(SO_x)_y$	$3.66 \cdot 10^{-2}$	1.02 (dioxane)	76.8
9**	$AlCl_3 \cdot 6H_2O$	$Al_{0.09}Ti_{0.93}O_{2-\delta-x}Cl_x$	$<10^{-5}$	0.84	79.6
10**	**10a**	$P_{0.07}Ti_{0.94}O_{2-\delta}$	$0.9 \cdot 10^{-4}$	0.78	80.6

* Selectivity (%) for DEG based on EG for the initial molar ratio EO : EG = 1 : 2.
** See Ref. 7.

prepared previously [7] exhibit extremely low catalytic activities. The rate constant for oxyethylation in the presence of the phosphorus titanate system synthesized from 4-ethyl-2,8,6-trioxaphosphabicyclo[2.3.2]octane (**10a**) (specimen **10**), which, according to a previous publication,[7] virtually does not contain acid sites, exceeds appreciably the value found for specimes **5** and **9**. In the presence of phosphorus titanate systems prepared using copper bromide complexes with phosphoramidites (specimens **3** and **4**), the rate constant for the catalytic reaction increases by an order of magnitude. As can be seen in Table 1 (specimen **7**), the rate constants are low in the presence of copper bromide. The highest activity in oxyethylation is observed for the systems prepared from phosphoramidite precursors (specimens **1** and **2**). In the presence of these systems, the rate constant is not lower than that on the most active heterogeneous catalyst for alcohol oxyethylation, $LaPO_4$, where it amounts to $1.3 \cdot 10^{-3}$ L g^{-1} min^{-1} at 115 °C.[16] The system based on $Al_2(SO_4)_3$ (specimen **8**) is as active in oxyethylation as the phosphoramidite specimens. However, in this case, as in the presence of other known acid catalysts, ~0.1% by-product, dioxane, is formed for equimolar initial amounts of EG and EO. Yet another important distinction of phosphorus titanate systems from sample **8** is the much higher selectivity with respect to the lower homolog, DEG. For phosphorus titanate and copper phosphorus titanate oxides, the *C* value is 0.37—0.52, which corresponds to 85—89% selectivity of DEG formation for an initial EO : EG molar ratio of 0.5. For comparison, the patented heterogeneous catalyst of oxyethylation, which is the ZSM-5 zeolite modified by potassium hydroxide, ensures a formation selectivity for the first product of <80% ($C = 0.82$) under the same initial conditions.[17] It is noteworthy that in the presence of all phosphorus titanate oxides exhibiting high activity in oxyethylation, no dioxane is formed.

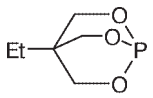

10a

Previously,[7,8] it was shown that the conditions of synthesis of phosphorus titanate systems based on etriol phosphite influence the acid-base properties of the surface, the specific surface area, and the total adsorption volume but not the averaged pore volume or pore distribution. These oxides are characterized by a homogeneous distribution of pores with a size of 8—10 Å when calculated for a slit-like configuration. Table 2 presents data on the porous structure of the oxides based on new phosphorus titanate precursors. For comparison, the same Table shows characteristics of the porous structure determined previously[7] for samples **9** and **10**. It can be seen that the average pore size for the phosphorus titanate system based on phosphoramidite is also 8—10 Å, although the adsorption volume increases to 3.4 mmol g^{-1}, and the specific surface area reaches 160 m^2 g^{-1}. For the copper phosphorus titanate oxides (specimens **3** and **4**), the average pore size is 18—20 Å, which is nearly equal to the value[7] found for the aluminum-containing oxide (specimen **9**).

The linear section of the relative adsorption isotherm (Fig. 1), which allows one to estimate the homogeneity of pore distribution, indicates that specimen **2** contains no micropores with sizes of <10 Å, and specimen **3**, of <18—20 Å. The pattern of the relative adsorption isotherm for specimen **1** is identical to those for specimens **2** (see Fig. 1) and **10** (see Ref. 7). This indicates that the change in the pore size in specimen **3** is largely caused by incorporation of copper ions in the structure.

A homogeneous pore structure and a narrow pore size distribution are also indicated by the theoretical adsorption plots that represent the variation of the adsorption volume *vs.* the number (*n*) of adsorbed layers of the sorbate (Fig. 2). Figure 2 also shows the adsorption isotherms for the oxides studied previously.[7,8] It can be seen that these plots have only one break for any of the titanates studied, pointing to a narrow pore size distribution. The difference between the porous structures is that the break corresponds to $n = 2$ for phosphorus titan-

Table 2. Selected parameters of the porous structure (from BET) and X-ray diffraction data for compounds **1—5**, **9**, and **10**

Specimen	Porous structure parameters			X-Ray diffraction			
	S_{sp}/m^2 g^{-1}	V_{ads}/cm^3 g^{-1}	*r*/nm	*c*/nm	*D*/nm	$\varepsilon \cdot 10^{-3}$	*K*
1	91	0.11	0.8	0.945	7.7	0.29	15.7
2	160	0.12	0.9	0.941	7.6	6.84	30.6
3	85	0.15	1.9	0.944	10.5	1.89	12.8
4	93	0.26	1.8	0.945	12.9	2.39	14.1
5	3.2	0.009	3	0.947	39.7	0.3	0.5
9*	82	0.18	1.9	0.942	9.6	1.23	14.2
10*	83	0.082	0.9	0.941	8.2	3.12	14.8

* See Ref. 7.

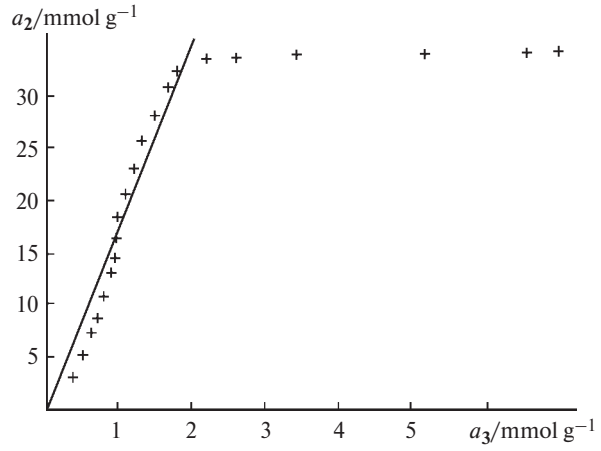

Fig. 1. Comparative plot for nitrogen adsorption on specimens **2** (a_2) and **3** (a_3).

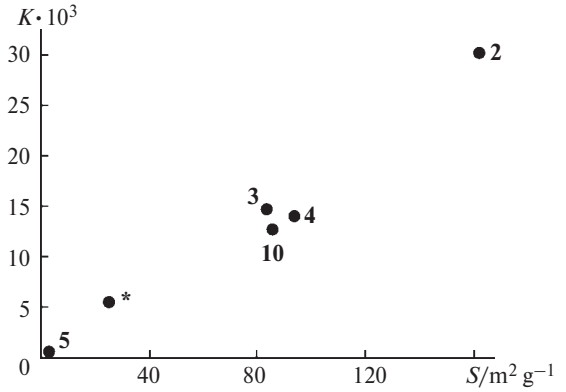

Fig. 3. Correlation between the specific surface area (S) and the fine structure factor (K) for specimens **2—5**, **10** and the specimen (marked by an asterisk) prepared[4] from etriol phosphite without chelation ($P_{0.07}Ti_{0.94}O_{2-\delta}$).

ate oxides, whereas for specimens containing aluminum and copper ions, $n = 4$. Thus, the inclusion in titanium oxides of metal heteroatoms, characterized by greater ionic radii than phosphorus, results in greater pore size without reducing significantly the homogeneity of the porous structure as a whole.

X-Ray diffraction and EXAFS studies of the fine structures of the copper titanium oxides prepared by alkoxo synthesis[18] showed that the Cu^{2+} ions grow epitaxially the titanium oxide microcrystallites in the tetragonal orientation of anatase, thus inducing termination of the microcrystallite growth. The pores might be formed predominantly in the local sites of this termination. Since heteroatoms (Cu and P) are joined within the framework of a single structure, distortions of the long-range order in the anatase lattice occur most likely at the same positions, and the pore size distribution does not change significantly.

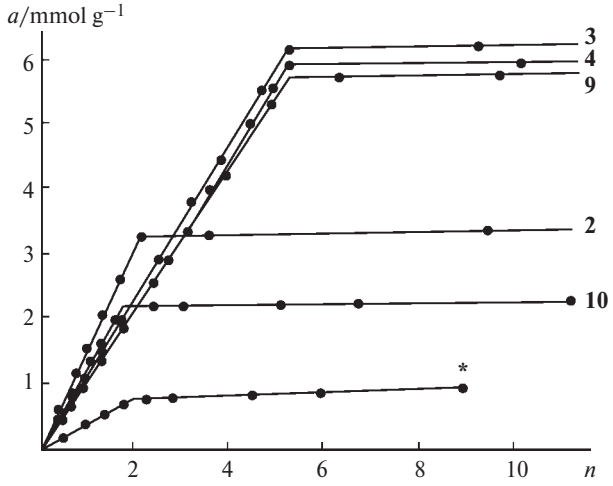

Fig. 2. Nitrogen adsorption (a) on the phosphorus titanate oxides *vs.* the number of adsorbed layers of molecules (n) for specimens **2—4**, **9**, **10** and the specimen (marked by an asterisk) prepared[4] from etriol phosphite without chelation ($P_{0.07}Ti_{0.94}O_{2-\delta}$).

It can be seen from X-ray diffraction data (see Table 2) that the introduction of phosphorus results in a pronounced increase in the microcrystallite dispersity compared to that in nonmodified titanium oxide. The fine structure factor $K = I/D \cdot \varepsilon^{-3}$ (I is reflection intensity, D is the averaged size of a microcrystallite, ε is a structure microdistortion factor) adequate to the surface geometry is proportional to the BET specific surface area for any of the phosphorus-containing oxides (Fig. 3). This shows that all the phosphorus titanate oxides prepared from phosphite precursors by the alkoxo method are characterized by highly organized structures with not only a homogeneous pore distribution but also a homogeneous size distribution of microcrystallites.

Previously, it has been shown using TPD of ammonia that specimen **10** prepared from etriol phosphite contains virtually no acid sites.[7] According to XANES data, the local charge state of titanium atoms in this specimen implies an increased electron density.[8] Thus one may have expected that the use of phosphoramidite compounds, which are stronger Lewis bases, would increase the base properties of titanium oxides.

Table 3 contains the activation energy distribution of the acid sites derived from the TPD data for ammonia. It can be seen that, contrary to expectations, the oxides based on phosphoramidites possess clear-cut acid properties. The strength of the acid sites was assigned according to known published data.[19,20] It can be seen from Table 3 that the nature of precursors affects appreciably the number and strength of the acid sites. When phosphoramidites are used, the chemisorption capacity relative to ammonia markedly increases at high temperatures (550—600 °C). Some of ammonia is chemisorbed irreversibly, resulting apparently in surface amination.

Table 3. Activity in oxyethylation and active site distribution over the activation energies of ammonia thermodesorption (kJ mol^{-1})

Specimen	a_0[a] /μmol g^{-1}	S_j[b]			$k_0[p(r)]_{exp}$[c] /kg (g min)$^{-1}$
		1[d]	2[e]	3[f]	
1	386	67	306	13	0.013
2	354	69	248	37	0.037
3	324	71	249	4	0.003
4	300	78	222	0	0.003
8	660	148	493	19	0.015
9[g]	177	34	126	17	0.007

[a] Total acidity over all regions.
[b] The number of acid sites of an *j*th region having a particular activation energy of ammonia desorption E_d, which characterizes the strength of acid sites in each region.
[c] Experimental rate constants.
[d] $E_d < 90$ kJ mol^{-1}.
[e] 90 kJ mol$^{-1} < E_d < 130$ kJ mol^{-1}.
[f] $E_d \leq 130$ kJ mol^{-1}.
[g] See Ref. 7.

The TPD data for CO_2, used as a probe molecule in investigations of the base properties of the surface (Fig. 4), show that the initial TiO_2 is responsible for a set of diffuse peaks in the temperature range in which the TPD of ammonia has revealed[8] a diffuse region of acid sites. Apparently, the CO_2 desorption region corresponds to medium-strength Lewis sites, which may be represented by μ-O bridges connecting positively charged Ti^{4+} ions and having a partial negative charge. Specimen **8** prepared by treatment of the gel surface with $Al_2(SO_4)_3$ and having a high concentration of acid sites (see Table 3) almost does not contain base sites (see Fig. 4).

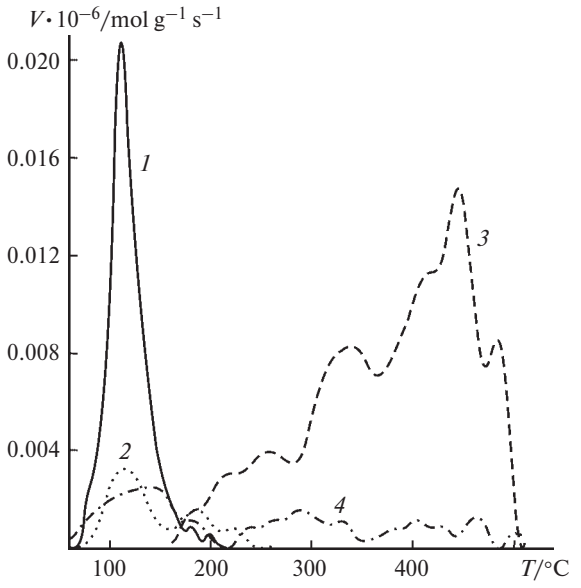

Fig. 4. TPD of adsorbed CO_2 for specimens **1** (*1*), **2** (*2*), **5** (*3*), and **8** (*4*); *T* is the desorption temperature, *V* is the volume of desorbed CO_2.

This result suggests that treatment of the gel surface leads to sulfonation giving rise to the Brønsted acid sites.

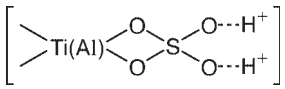

The TPD spectra of phosphorus titanate oxides (specimens **1** and **2**) prepared from phosphoramidite precursors exhibit a rather sharp peak of CO_2 desorption in the region of 114 °C. Despite the relatively low CO_2 chemisorption, the narrow peak attests to homogeneity of the base sites. In all probability, these are O atoms in the phosphorus titanate fragments of the structure.

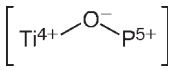

Thus, TPD data show that the incorporation of phosphorus from phosphoramidites markedly increases the strength of acid sites. The XANES data point to an increase in the positive charge in the local environment of Ti atoms relative to that in the nonmodified oxide.[21] In view of the fact that the phosphorus-containing system is a single phase, by analogy with the known views on the formation of semiconductor materials, one can suggest that the P atoms generate impurity levels, thus leading to a higher concentration of positively charged vacancies in the titanium d-band.[22]

Previously,[23] etriol phosphite was found to remain virtually unchanged throughout the sol-gel transformations of the chelated alkoxide complex up to the formation of a solid gel. Hence, it was assumed[23] that the P^{III} atom in etriol phosphite reacts with the surface chelate groups and suppresses the Lewis acid sites. Conversely, phosphoramidites undergo alcoholysis even in the initial solution, and after addition of aqueous alcohol, they are hydrolyzed to give a four-coordinate P^{III} atom in the hydrated phosphite, and the hydrated phosphites condense with titanium oxo hydroxo butoxide. At a subsequent stage, during the gel heat treatment, further oxidation of P^{III} to P^{V} probably takes place, which may be responsible for the higher acidity of the system.

To elucidate the role of acid sites catalyzing the EG oxyethylation, we used regional rate analysis, which provides correlations between the number and strength of the acid sites on the catalyst surface and their activity in heterogeneous catalytic reactions.[24,25] To this end, the acidity spectra were split into regions according to the strength of acid sites (see Table 3). In terms of the regional rate method, the overall reaction rate on the catalyst reduced to unit weight is represented as the sum over all regions of the products of the regional rate in this

region by the number of acid sites in this region. The regional rate is also a function of the reagent partial pressure[24]

$$V_i(r) = \sum_{j=1}^{3} k_{0j}[p(r)]S_{ij},$$

where k_{0j} is the specific regional rate constant in an jth region; S_{ij} is the number of acid sites in the jth region on an ith catalyst (μmol g^{-1}).

Since the number of regions ($n = 3$) is smaller than the number of catalysts ($N = 6$), the specific regional rate constants averaged over all specimens were calculated using the least-squares method by minimizing the functional

$$\Phi = \sum_{i=1}^{N}(k_0[p(r)])_i - \sum_{j=1}^{3} k_{0j}[p(r)]S_{ij}.$$

The correlation quality was characterized by the correlation coefficient R, calculated to be 0.88 with allowance for the number of degrees of freedom. The mean-square error of approximation $\sigma = 0.5\%$. The input data and the results of calculations are listed in Table 3. The $k_{0j}[p(r)]$ values are as follows: $k_{01}[p(r)] = 0.085 \cdot 10^{-4}$, $k_{02}[p(r)] = 0.031 \cdot 10^{-4}$, and $k_{03}[p(r)] = 8.7 \cdot 10^{-4}$.

The results imply the presence of a correlation between the catalyst activity and the catalyst acidity spectra. Comparison of the $k_{0j}[p(r)]$ values shows that the reaction proceeds almost exclusively at strong acid sites (region 3) characterized by activation energies of ammonia desorption $E \geq 130$ kJ mol^{-1}. The known averaged specific regional rate constants were used to calculate the rate constants for each catalyst. Comparison of experimental and calculated rate constants for all specimens is shown in Fig. 5. It can be seen that fairly good agreement between the experimental and calculated values is attained for catalysts characterized by high concentrations of strong acid sites.

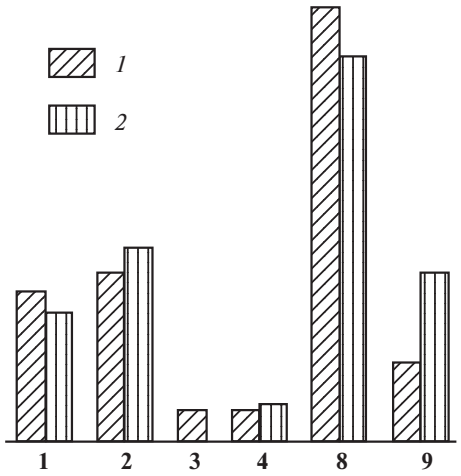

Fig. 5. Diagram of experimental (*1*) and calculated (*2*) rate constants for oxyethylation of EG (regional rate method) depending on the concentration of strong acid sites for specimens **1—4**, **8**, and **9**.

This may imply that the rate-determining step in the oxyethylation mainly involves the strong aprotic acid sites of titanate oxides. The base sites activate, apparently, the alcoholic group and thus ensure concerted acid-base catalysis on the catalyst surface (which is typical[26] of the catalysis of EO reactions by metal oxides). On the basis of the foregoing, the following scheme for the reactant activation can be proposed (Scheme 1).

Scheme 1

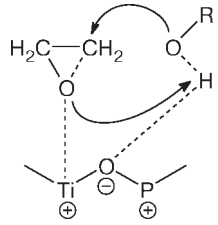

Thus, phosphorus titanate oxides with a homogeneous distribution of supermicropores containing Lewis base (medium-strength) and acid (strong) sites ensure high activity and selectivity of the oxyethylation of ethylene glycol. The dimensions of cavities represented by homogeneous supermicro- and small mesopores in the phosphorus-titanate oxides restrict the process propagation and prevent an increase in the sizes of molecules of reaction products; *i.e.*, the sieve effect is involved in the catalytic reaction.

This work was financially supported by the Russian Foundation for Basic Research (Project No. 00-03-32407a) and the Presidium of the Russian Academy of Sciences (Project "Nanocluster and supramolecular compounds").

References

1. N. Schonfeldt, *Grenzflachenaktive Athylenoxid-Addukte*, Wissenschaftliche Verlagsgesellschaft MBH, Stuttgart, 1976.
2. L. G. Lundsted and I. R. Schmolka, *Block and Graft Copolymerization*, **2**, Ed. R. J. Ceresa, J. Wiley and Sons, New York, 1976.
3. N. Manolova, J. Libiszowski, R. Szumanski, and S. Penszek, *Polym. Int.*, 1995, **36**, 23.
4. N. M. van Os, in *Nonionic Surfactants, Surfactant Science Series*, **72**, Marcel Dekker, Inc., New York, 1998, 22.
5. N. N. Lebedev, V. P. Savel´yanov, and Yu. I. Baranov, *Zh. Prikl. Khim.*, 1969, **42**, 1815 [*J. Appl. Ghem. USSR*, 1969, **42** (Engl. Transl.)].
6. N. M. van Os, in *Nonionic Surfactants, Surfactant Science Series*, **72**, Marcel Dekker, Inc., New York, 1998, 5.

7. M. V. Tsodikov, O. V. Bukhtenko, E. V. Slivinskii, L. N. Slastikhina, A. M. Voloshchuk, V. V. Kriventsov, and L. E. Kitaev, *Izv. Akad. Nauk, Ser. Khim.*, 2000, 1829 [*Russ. Chem. Bull., Int. Ed.*, 2000, **49**, 1803].
8. M. V. Tsodikov, E. V. Slivinskii, V. V. Yushchenko, L. E. Kitaev, V. V. Kriventsov, D. I. Kochubei, and A. T. Teleshev, *Izv. Akad. Nauk, Ser. Khim.*, 2000, 2037 [*Russ. Chem. Bull., Int. Ed.*, 2000, **49**, 2003].
9. E. E. Nifant´ev, *Khimiya fosfororganicheskikh soedinenii* [*Chemistry of Organophosphorus Compounds*] Izd-vo MGU, Moscow, 1971, 352 pp. (in Russian)
10. A. T. Teleshev, G. M. Grishina, A. A. Borisenko, N. N. Nevskii, and E. E. Nifant´ev, *Zh. Org. Khim.*, 1984, **54**, 1710 [*J. Org. Chem. USSR*, 1984, **54** (Engl. Transl.)].
11. V. F. Shvets and N. N. Lebedev, *Kinetika i Kataliz*, 1968, **9**, 504 [*Kinet. Katal.*, 1968, **9** (Engl. Transl.)].
12. B. Weibull and B. Nycander, *Acta Chem. Scand.*, 1954, **8**, 847.
13. S. S. Gorelik, L. N. Rastorguev, and Yu. A. Skakov, in *Rentgenograficheskii i elektronooptícheskii analiz* [*X-Ray Diffraction and Electrooptical Analysis*], Metallurgiya, Moscow, 1970, 83; 145 (in Russian).
14. R. Ch. Mikhail, S. Brunauer, and E. E. Bodor, *J. Colloid Interface Sci.*, 1968, **26**, 45; 54.
15. V. V. Yushchenko, *Zh. Fiz. Khim.*, 1997, **71**, 628 [*Russ. J. Phys. Chem.*, 1997, **71** (Engl. Transl.)].
16. US Pat. 5,057,627, 1991; *Chem. Abstrs.*, 1991, **111**, 231451z.
17. US Pat. 5256828, 1993; *RZhKhim.*, 1995, 2N149P.
18. M. V. Tsodikov, Ye. A. Trusova, Ye. V. Slivinskii, G. G. Hernandez, D. I. Kochubey, V. G. Lipovich, and J. A. Navio, *Studies in Surface and Catalysis*, 1998, **118**, Eds. B. Delmon and J. T. Yates, Lonvain-la-Neuve, Belgium, 679.
19. A. Aurox and A. Gervasini, *J. Phys. Chem.*, 1990, **94**, 6371.
20. N. Y. Chen, W. W. Kaeding, and F. G. Dwyer, *J. Am. Chem. Soc.*, 1979, **101**, 6783.
21. M. V. Tsodikov, O. V. Bukhtenko, T. N. Zhdanova, I. A. Litvinov, L. E. Kitaev, L. N. Vasil´eva, and V. V. Kriventsov, *Aktual´nye problemy neftekhimii* [*Current Problems of Petroleum Chemistry*] (*Moscow, April 17—20, 2001*), *Abstrs.,* Moscow, 2001, 194 (in Russian).
22. Ch. A. Wert and R. M. Thomson, *Physics of Solids*, McGray-Hill Book Company, New York—San Francisko—Toronto—London, 1964, 543 pp.
23. A. T. Teleshev, L. N. Vasil´eva, E. E. Nifant´ev, M. V. Tsodikov, O. V. Bukhtenko, and T. N. Zhdanova, *Aktual´nye problemy neftekhimii* [*Current Problems of Petroleum Chemistry*] (*Moscow, April 17—20, 2001*), *Abstrs.,* Moscow, 2001, 106 (in Russian).
24. Y. Yoneda, *J. Catal.*, 1967, **9**, 51.
25. V. V. Yushchenko and B. V. Romanovskii, *Zh. Fiz. Khim.*, 1999, **73**, 646 [*Russ. J. Phys. Chem.*, 1999, **73**, No. 4 (Engl. Transl.)].
26. K. Yamaguchi, K. Ebitani, T. Yoshida, H. Yoshida, and K. Kaneda, *J. Am. Chem. Soc.*, 1999, **121**, 4526.

Received October 15, 2001;
in revised form January 24, 2002